

How is surface ozone in Europe linked to Asian and North American NO_x emissions?

R.G. Derwent^{a,*}, D.S. Stevenson^b, R.M. Doherty^b, W.J. Collins^c, M.G. Sanderson^c

^a *rdscientific, Newbury, Berkshire RG 14 6LH, United Kingdom*

^b *Institute for Atmospheric and Environmental Science, University of Edinburgh, United Kingdom*

^c *Met Office, Exeter, Devon, United Kingdom*

ARTICLE INFO

Article history:

Received 16 March 2008

Received in revised form 12 June 2008

Accepted 17 June 2008

Keywords:

Source–receptor relationships

Intercontinental transport

Tropospheric ozone

NO_x emissions

ABSTRACT

Source–receptor relationships linking North American and Asia NO_x emissions with surface ozone in Europe have been explored using a global Lagrangian chemistry–transport model. We used the model to perform a set of simulations, each 21 months in duration, which were comprised of a base case and a series of emission perturbation experiments. In each of the perturbation runs, an additional month-long NO_x emission pulse from a particular 10° × 10° region was included. Overall, results from 42 different emission regions in both boreal summer and winter were analysed. Shortly after the start of each NO_x emission pulse, increased ozone mixing ratios were detected at surface sites across Europe. The extra ozone peaked and then decayed away to leave a small but persistent ozone deficit that persisted throughout the year-long model experiments. The ozone responses varied spatially by over three orders of magnitude, depending on the location of the NO_x emission pulses in each continent and on the receptor location within Europe. Source–receptor relationships also varied markedly with season. NO_x emissions from lower latitudes, especially in the boreal summer, were found to decrease European ozone, when both the short- and long-term responses were considered. In this study, it has been possible to begin the process of examining the likely influences on ozone levels across Europe resulting from precursor emission controls in North America and Asia and, in turn, their possible impacts on meeting ozone air quality targets over Europe.

© 2008 Elsevier Ltd. All rights reserved.

1. Introduction

Source–receptor relationships have generally been employed to quantify the relationships between emission sources and air concentrations or deposition fluxes (Venkatram and Karamchandani, 1986). For example, source–receptor relationships have been described for sulphur deposition over Asia (Arndt and Carmichael, 1995), visibility over North America (Gebhart et al., 2000), particulate sulphate over Europe (Stohl, 1996), acid precipitation over France (Charron et al., 2000) and for acid precipitation

within the international convention on long-range transboundary air pollution (CLRTAP) (Bartnicki, 2000). Source–receptor relationships expressed as, for example, ppb at a receptor per unit source emission, are seen as an entirely different concept to source apportionments, source contributions or source attributions (Venkatram and Karamchandani, 1986). Since ozone O₃ formation is well understood to be an inherently non-linear chemical system, the source–receptor relationships generated here may be entirely different to the continental source attributions previously generated for O₃ in Europe (Derwent et al., 2004).

Attention has been given to the mechanisms by which O₃ precursor emissions from one continent may give rise to increased O₃ over another. Parrish et al. (1993) were the

* Corresponding author.

E-mail address: r.derwent@btopenworld.com (R.G. Derwent).

first to suggest that tropospheric O₃ levels in Europe may be influenced by export from the North American continent. Trans-Atlantic pollution transport has been associated with mid-latitude cyclones and their warm conveyor belts, post cold front airstreams and low-level flows (Stohl and Trickl, 1999; Cooper et al., 2001; Stohl, 2001). Li et al. (2005) described the major outflow pathways for North American pollution to the North Atlantic region in summer. Auvray and Bey (2005) describe how North American O₃ enters Europe in the upper troposphere during the summer and how low-level flow is only important in spring. Lelieveld et al. (2002) and Li et al. (2005) address the flow from Asian sources into Europe through the influence of the summer monsoon.

Here, we use source–receptor matrices to quantify the link between European O₃ and Asian and North American NO_x emissions and show how they differ between summer and winter. The aim is to identify whether there are regional differences within these continents in the strength of intercontinental O₃ formation and transport. Such regional differences may have important repercussions for policy because trans-Atlantic O₃ transport exerts a significant external influence on European air quality (Derwent et al., 2006). Global scale O₃ precursor emissions and their controls are not currently taken into account in policy formulation within Europe under the European Union Clean Air for Europe (CAFE) Programme (Commission of the European Communities, 2005).

2. Description of the climate-chemistry model STOCHEM

STOCHEM is a global Lagrangian tropospheric chemistry-transport model, originally described by Collins et al. (1997). In the work described here, an early version of the model was employed in which the atmosphere is divided into 50,000 constant mass air parcels that are mapped after each advection time-step to a 5° by 5° resolution grid with nine vertical layers up to 100 hPa. Meteorological data in the form of analysis fields were provided at 6-hourly intervals by the Met Office numerical weather prediction models with a resolution of 1.25° longitude and 0.83° latitude and on 12 vertical levels, extending to 100 hPa. The advection time-step is 3 h. Turbulent mixing in the boundary layer is achieved by randomly re-assigning the vertical co-ordinates of air parcels over the depth of the boundary layer height. Small-scale convective processes are treated by randomly mixing a fraction of the air parcels between the surface and the cloud top, depending on the convective cloud top, convective cloud cover and convective precipitation rate. The chemical scheme includes 70 species that take part in 174 chemical reactions and utilises a time-step of 5 min.

Emission fields for a wide range of man-made trace gases including CH₄, CO, NO_x and VOCs for the year 2000 were taken from Cofala et al. (2007). Vegetation emissions of isoprene were set at 500 Tg yr⁻¹, lightning NO_x emissions 5.0 Tg N yr⁻¹ and aircraft emissions 0.5 Tg N yr⁻¹. The SO₂ and NO_x emissions from international shipping were based on 1995 data with an assumed growth rate of 1.5% per year between 1995 and 2000 (Dentener et al., 2005). The total of

the emissions of methane from wetlands, tundra and rice paddies was set at 260 Tg yr⁻¹ as detailed in Collins et al. (1999). After each advection time-step, the surface emissions are distributed equally over all the Lagrangian cells that are within the boundary layer for a particular grid square. If there are no cells within the boundary layer for a particular grid square then the emissions are stored until a cell passes through.

In previous work, Collins et al. (1997, 1999) have described comparisons of model results with observations for OH, O₃, NO_x and HO_x species. Stevenson et al. (2002) compared the model O₃ concentrations with surface observations for 96 remote locations in Europe. Furthermore, the methane lifetime due to OH removal was found to be 9 yr in agreement with Prinn et al. (1995) and multi-model results (Stevenson et al., 2006). The global ozone budgets, burdens and turnover times are well within the ranges in the literature (Collins et al., 2000).

3. Chemistry-transport model experiments

The STOCHEM model has been used to study the formation and intercontinental transport of ozone from Asian and North American NO_x emissions to Europe. The transient behaviour of O₃ in response to emission pulses of NO_x was investigated by starting the model from an initial set of trace gas mixing ratios on 1st October 1997 and using analysed wind fields to run through to 30th June 1999. Several repeat experiments were conducted with this set-up: firstly a base case, then a series of 84 integrations, which differed from the base case only in that an additional pulse of NO_x emissions was included in specific regions of Asia or North America (see Fig. 1 for the locations), for 1 month periods beginning in either January or July 1998. Differences in trace gas mixing ratios between each experiment and the base case were analysed. NO_x emission pulses of 0.2 Tg N were added in each of 21 10° × 10° latitude–longitude regions across Asia and emission pulses of 0.1 Tg N were added in each of 21 10° × 10° latitude–longitude regions across North America. This was done for the months of January and July 1998 to examine differences in formation and intercontinental transport of O₃ during different seasons. The NO_x emission pulse sizes were arbitrary, being large enough to generate discernible differences but small enough to keep them in the linear range. The pulse sizes used for each continent were chosen so that they gave roughly the same O₃ responses in Europe and the results were scaled linearly to 0.1 Tg N per month. Linearity checks were performed as described below.

Since STOCHEM is a Lagrangian chemistry-transport model, we have access not only to standard gridded fields of mixing ratios but also to Lagrangian mixing ratios carried by individual air parcels. In this study, much of the analysis has been performed using these air parcel mixing ratios. At the end of each 3-h advection time-step, the trace gas mixing ratios held by all air parcels within a region defined by a solid angle of 1° radius around each location of interest were stored. When the model experiments were repeated, having changed only the NO_x emission fields, the air parcels took exactly the same paths through the model domain. However, each air parcel carried slightly different mixing

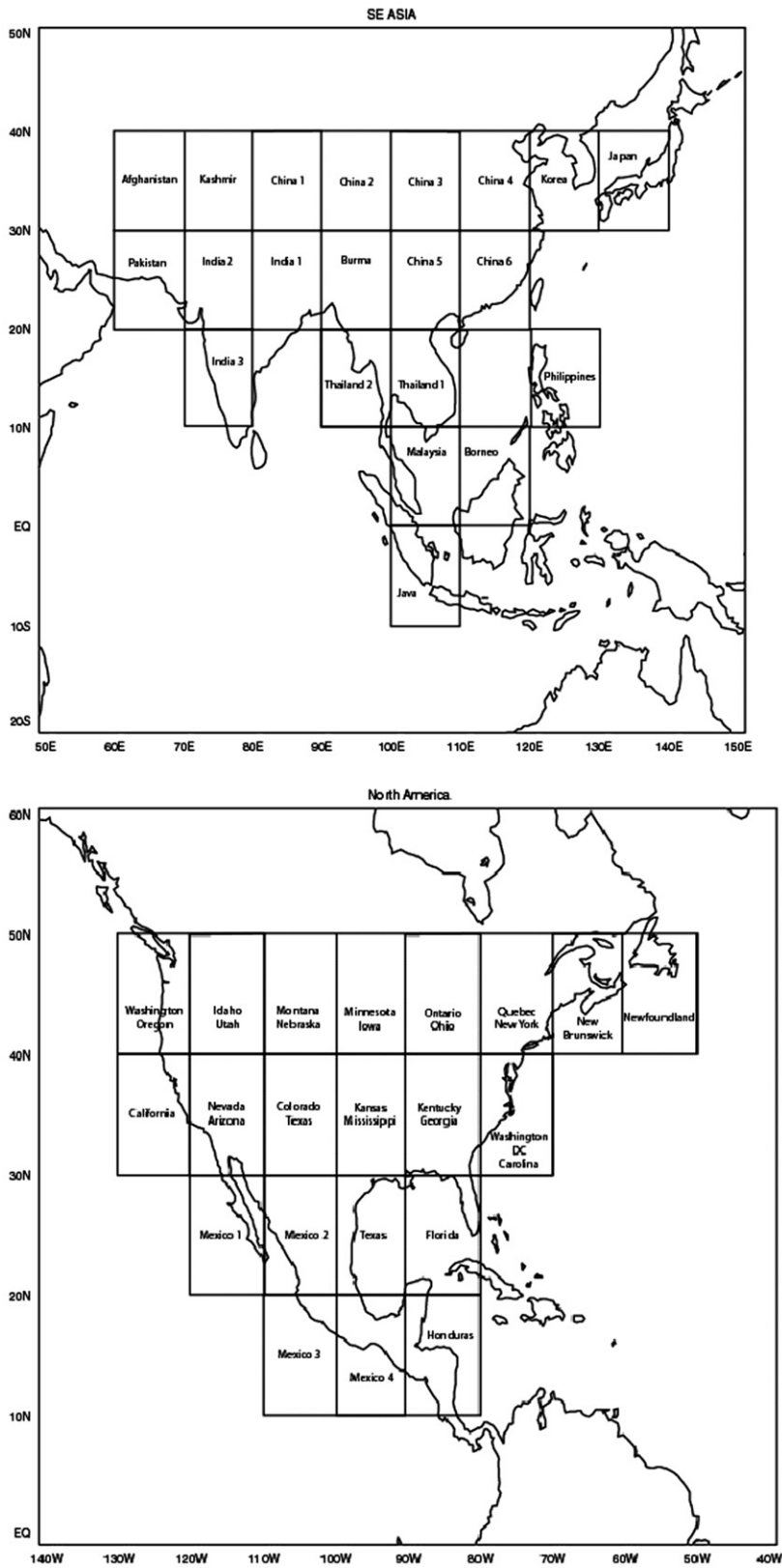


Fig. 1. The locations of the grid boxes used in the pulse experiments.

ratios in response to the emission changes. Differences between the air parcel mixing ratios in each of the emission perturbation experiments and the base case simulations were calculated and were used to evaluate source–receptor relationships. In all cases, only air parcels arriving in the atmospheric boundary layer in Europe have been considered in the analyses below. Peak O_3 responses and time-integrated responses were determined to elucidate both the short-term and the longer-term equilibrium responses.

3.1. Intercontinental O_3 formation and transport from Asia to Europe

Shortly after the start of the Asian NO_x emission pulses, increases in modelled ozone mixing ratios were detected at the surface at Mace Head, Ireland, which is a baseline atmospheric monitoring site situated on the Atlantic Ocean coastline. Mace Head is used here because of its importance in the monitoring of air masses entering North West Europe (Simmonds et al., 2004). The timing of the arrival of the extra or excess ozone and its magnitude depended on the location of the emission pulse. Fig. 2 shows the modelled surface excess O_3 at Mace Head with the January pulses for a range of locations within Asia that form an approximate north–south transect, scaled to an emission pulse of 0.1 Tg N. The peak in the excess ozone of 0.27 ppb from the ‘China 3’ pulse (see Table 1 and Fig. 1) arrived after about 36 days from the start of the pulse whereas that from ‘Java’ was only about 0.02 ppb and arrived after 47 days. Table 1 contains a summary of all 21 Asian January pulse experiments and shows how O_3 responses characterised by their highest daily average mixing ratios, varied from 0.43 to 0.02 ppb, spanning a range of over 20 in magnitude, with emissions from the ‘Japan’ (most easterly) and the ‘Java’

(most southerly) grid-squares generating the largest and smallest responses, respectively.

Responses at Mace Head showed evidence of some systematic geographical influences depending on the location of the emission pulse. There was a clear latitudinal gradient from north to south with the largest responses produced by pulses emitted further north. Systematic east–west gradients were not apparent, in general, but there were significantly increased responses that could be explained by orographic lifting of surface pollution in the proximity to the Himalayas (see entry for ‘Afghanistan’, Table 1) and to the regions where Asian air masses flow out into the Pacific Ocean (see entry for ‘Japan’, Table 1). However, their latitudes are closest to that of Mace Head, Ireland (53° N) and this may be the overriding influence.

O_3 responses peaked after a short while, about 30–40 days, then began to decay away towards zero. After about 3–5 months they changed sign and small but consistent deficits of up to 5 ppt were found in each model experiment, see Fig. 2. The negative responses were about one to two orders of magnitude smaller than the peak positive responses. The negative responses appeared to decay away but this is partly an artefact because they exhibited significant seasonal cycles. When the model experiments were followed over extended periods, for example, for 4 yr as in Derwent et al. (2001), pronounced seasonal cycles were observed with the amplitude of each successive cycle progressively reducing. The e-folding time of this negative O_3 response was found to be similar to that of the methane CH_4 deficit and to be comparable to the global CH_4 adjustment time of about 11 yr (Wild et al., 2001; Stevenson et al., 2004).

Analysis of the differences in the reaction fluxes between the pulse experiments and the base case model experiment, revealed the origin of the excess O_3 found in

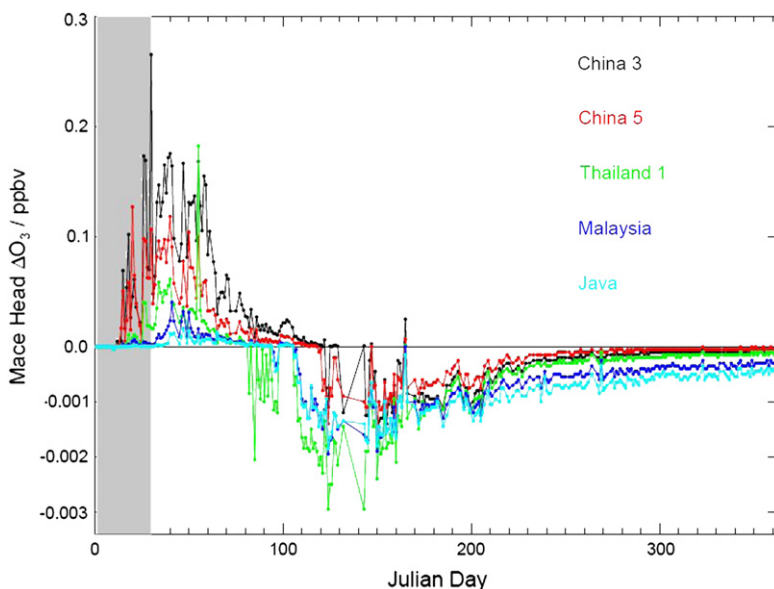


Fig. 2. Ozone responses (ppb) in the model surface layer at Mace Head from 1st January 1998 onwards following month-long (January 1998 – shaded) pulses of NO_x emissions emitted from five different $10^\circ \times 10^\circ$ grid-squares in a north–south transect through Asia (see Fig. 1 for locations). N.B. the negative ozone responses are on a scale 50 times more sensitive than the initial positive responses.

Table 1

Peak ozone and time-integrated ozone responses at Mace Head, Ireland to Asian NO_x emission pulses emitted in January

Region	Latitude	Longitude	Peak O ₃ response, ^{a,b} ppb	Time-integrated ozone response, ^a ppb months		
				Positive phase	Negative phase	Net
Afghanistan	30°–40°	60°–70°	0.39	0.27	–0.05	0.21
Kashmir		70°–80°	0.33	0.26	–0.05	0.21
China 1		80°–90°	0.30	0.31	–0.07	0.24
China 2		90°–100°	0.36	0.30	–0.06	0.23
China 3		100°–110°	0.27	0.22	–0.04	0.18
China 4		110°–120°	0.20	0.15	–0.03	0.13
Korea		120°–130°	0.24	0.19	–0.04	0.15
Japan		130°–140°	0.43	0.28	–0.07	0.22
Pakistan	20°–30°	60°–70°	0.16	0.12	–0.04	0.08
India 2		70°–80°	0.06	0.05	–0.02	0.03
India 1		80°–90°	0.12	0.10	–0.02	0.07
Burma		90°–100°	0.14	0.12	–0.03	0.09
China 5		100°–110°	0.13	0.12	–0.02	0.10
China 6		110°–120°	0.20	0.10	–0.02	0.08
India 3	10°–20°	70°–80°	0.04	0.02	–0.03	–0.01
Thailand 2		90°–100°	0.04	0.02	–0.03	–0.02
Thailand 1		100°–110°	0.18	0.05	–0.05	0.00
Philippines		130°–140°	0.09	0.05	–0.05	0.00
Malaysia	0°–10°	100°–110°	0.04	0.02	–0.08	–0.06
Borneo		110°–120°	0.04	0.02	–0.07	–0.05
Java	10°S–0°	100°–110°	0.02	0.007	–0.11	–0.10
Average			0.18	0.13	–0.05	0.08

^a Results scaled to NO_x emission pulses of 0.1 Tg N.

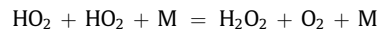
^b Highest daily mean excess mixing ratio.

the short-term at the surface at Mace Head to involve the stimulation of the flux through the NO + HO₂ reaction. The origins of the long-term ozone deficits involved the depletion of CH₄ through the OH + CH₄ reaction. Once the NO_x concentrations readjusted after the pulse (typically within a few months), the depleted CH₄ levels led to depleted O₃ production rates because CH₄ oxidation is an important source of tropospheric O₃.

By integrating over time, it is possible to quantify the equilibrium time-integrated O₃ responses by considering both the initial positive phase and the long-term negative phase. The time-integrations for the initial positive phase were carried out over the entire period of this phase, generally about 3 to 5 months, whereas those for the long-term phase were carried out for a sufficiently long enough time period so as to include all of the negative phase using the CH₄ adjustment (e-folding) time of 11 yr. Table 1 presents the time-integrated responses for the positive and negative phases, together with the net results, representing the overall responses. Time-integrated responses span a wide range from 0.007 to 0.31 ppb months for the positive NO_x-driven phase whereas those for the negative CH₄-driven phase span a much reduced range from –0.02 to –0.11 ppb months. For the emissions from mid-latitude grid-squares, the negative phase responses are small and of little consequence. However, for the tropical grid-squares the negative responses are comparable in magnitude to the positive responses. Hence, the two responses nearly cancel and the net time-integrated responses are close to zero. Because of the presence of a significant seasonal cycle in the CH₄-driven phase, the estimated negative time-integrated ozone responses are subject to considerable uncertainty.

In a further series of pulse experiments, the linearities of the O₃ responses to the signs and sizes of the NO_x emission pulses were checked. In each experiment summarised in Table 2, the NO_x emission pulse was applied during January and over the 10° longitude × 10° latitude region centred over 'Japan'. Experiments were performed with both negative emission pulses where NO_x emissions in the four selected STOCHEM 5° × 5° grid-squares were reduced below their base case values and with positive pulses as above. The signs and magnitudes of the pulses are given in Table 2. In the experiments with negative NO_x pulses, the responses of O₃ and CH₄ were exactly analogous to those with positive pulses, except with opposite signs.

Table 2 presents the peak O₃ and the time-integrated O₃ responses for the positive NO_x-driven and negative CH₄-driven phases, together with the net responses, scaled to a positive 0.1 Tg N per month emission pulse. They each showed consistent trends throughout the series of experiments irrespective of the sign of the emission pulses. Scaled O₃ responses steadily increased with decreasing NO_x emission pulse sizes. If the scaled responses had been independent of pulse size, the system would have been behaving linearly. Since this was not the case, the system showed some degree of non-linearity. The peak O₃ responses became relatively more sensitive as NO_x emissions were reduced. The origin of this non-linearity in the O₃ responses at low NO_x levels was found to be due to the competition between the following first order and second order radical loss processes as originally suggested by Lin et al. (1988):



However, for a range of positive pulse sizes varying by a factor of 32 in magnitude (see Table 2), we find scaled O₃ responses with a spread of ±20%, which represents the typical uncertainty due to our experimental design. For the rest of this study, we linearly scale our results to emission pulses of 0.1 Tg N per month, assume additivity and

Table 2

Variation in peak O₃ responses and scaled peak (in parentheses) and time-integrated O₃ responses at Mace Head, Ireland to Asian NO_x emission pulses of varying sizes and signs emitted in January

NO _x emission pulse, Tg N per month	Peak O ₃ response, ^{a,b} ppb	Time-integrated ozone response, ^c ppb months		
		Positive phase	Negative phase	Net
0.2	0.85 (0.43)	0.28	–0.07	0.22
0.1	0.48 (0.48)	0.32	–0.08	0.24
0.05	0.26 (0.53)	0.35	–0.09	0.26
0.025	0.14 (0.56)	0.37	–0.09	0.27
0.006	0.037 (0.59)	0.39	–0.12	0.27
–0.006	–0.044 (0.71)	0.49	–0.10	0.39
–0.012	–0.091 (0.73)	0.51	–0.11	0.40
–0.02	–0.14 (0.78)	0.53	–0.12	0.41

^a Highest daily mean excess mixing ratio.

^b Results in parentheses have been scaled to a positive month-long NO_x emission pulse of 0.1 Tg N emitted over 'Japan'.

^c Results have been scaled to a positive month-long NO_x emission pulse of 0.1 Tg N emitted over 'Japan'.

independence of sign, even though we know that this level of linearity is an approximation.

Significant seasonal variations were noted in the O₃ responses to the month-long Asian NO_x pulses, as indicated by a comparison of Table 1 with Table 3, which shows equivalent results for NO_x pulses emitted in July. The influence of the Himalayan mountain range was absent in the July pulse experiments, presumably because of the influence of the monsoon, leaving a clear gradient in response from 'Java' to 'Japan', and showing the dominant influence of outflow into the Pacific Ocean region rather than orography. Peak O₃ responses in the initial positive phase were between factors of 3 and 10 smaller in July compared with January, reflecting the shorter lifetime of O₃ in summer and the longer transport times.

Time-integrated responses also showed large seasonal variations. The CH₄-driven negative responses were twice as large for the July pulse compared to January. Cancellation between the positive and negative phases increased markedly, with the result that all the July pulse experiments gave negative total time-integrated responses, ultimately leading to less O₃ at Mace Head. This result is in contrast with the situation in January when the majority of the experiments led to more O₃ at Mace Head. Overall, these results indicate that in the long-term, tropical Asian NO_x emissions act to reduce European surface O₃. For emissions during July, this extends to emissions from all of Asia. It should be noted that these hypothetical experiments consider changes in NO_x emissions in isolation from other emissions that may also affect O₃, OH and CH₄. It is likely that changes in NO_x emissions may be accompanied

by changes in other emissions and to evaluate that total impact of emission changes, all species should be considered together as in, for example, Stevenson et al. (2006).

3.2. Intercontinental O₃ formation and transport from North America to Europe

The responses at the surface at Mace Head, Ireland to the month-long NO_x pulses emitted across North America were similar to those described above from Asia. The responses resulting from North American pulses were stronger and arrived more rapidly than those from Asia but showed the same features of an initial positive phase followed by a long-term negative phase. Table 4 presents the results from 21 pulse experiments involving month-long NO_x pulses of 0.1 Tg N emitted across North America during January. Peak O₃ responses spanned over a factor of 30 from close to 3.5 ppb from the 'Idaho–Utah' region to 0.1 ppb from 'Mexico'.

The responses showed a clear latitudinal gradient from the north to south with highest values in the north and lowest in the south of the region. There were no systematic east–west gradients. Instead, significant increased responses could be found in some regions in proximity to the Rocky Mountains (see 'Idaho–Utah' and 'Nevada–Arizona', Table 4) and in the regions associated with the outflow of air masses into the North Atlantic Ocean region (see 'Newfoundland' and 'Quebec–New York', Table 4). Significantly decreased responses were also associated with proximity to the Rocky Mountains (see 'Colorado–Texas', Table 4) suggesting a possible bi-polar influence of orography on the formation and intercontinental transport of O₃ to Europe from North America.

Time-integrated responses showed an initial positive NO_x-driven phase, the magnitude of which varied from 0.08 to 0.61 ppb months, and a long-term CH₄-driven negative phase which varied from –0.02 to –0.11 ppb months. Again, the long-term negative phases were unimportant except for the grid-squares in the tropical regions. In these regions, the negative and positive phases were comparable, resulting in near-cancellation and in some cases changing the sign of the net time-integrated responses from positive (producing more O₃ at Mace Head) to negative (producing less at Mace Head).

Significant seasonal variations were noted in the responses to the month-long North American NO_x pulses as indicated by the differences in the results for the January and July experiments in Tables 4 and 5, respectively. The significant influence of the Rocky Mountains on the January results was much reduced in July and was only evident in those from the 'Colorado–Texas' grid-square. In the July experiments, a significant west–east gradient was observed, with responses increasing steadily from 'Washington–Oregon' in the west to 'Newfoundland' in the east and from 'California' to 'Washington DC–North Carolina'. Such gradients were not seen in the January experiments. These increasing responses along west–east transects appear to reflect the decreased travel times for the pulses from the more easterly grid-squares. Travel time is more crucial during the summer compared to the winter because of the shorter O₃ lifetime.

Table 3

Peak ozone and time-integrated ozone responses at Mace Head, Ireland to Asian NO_x emission pulses emitted in July

Region	Peak O ₃ response, ^{a,b} ppb	Time-integrated ozone response, ^a ppb months		
		Positive phase	Negative phase	Net
Afghanistan	0.01	0.01	–0.08	–0.07
Kashmir	0.03	0.02	–0.09	–0.07
China 1	0.04	0.02	–0.12	–0.09
China 2	0.06	0.03	–0.10	–0.07
China 3	0.05	0.03	–0.08	–0.05
China 4	0.05	0.04	–0.07	–0.03
Korea	0.09	0.06	–0.08	–0.02
Japan	0.16	0.08	–0.11	–0.03
Pakistan	0.02	0.00	–0.10	–0.10
India 2	0.01	0.01	–0.10	–0.10
India 1	0.02	0.01	–0.12	–0.11
Burma	0.02	0.01	–0.15	–0.14
China 5	0.02	0.02	–0.13	–0.11
China 6	0.03	0.02	–0.10	–0.09
India 3	0.03	0.01	–0.12	–0.11
Thailand 2	0.02	0.01	–0.13	–0.13
Thailand 1	0.02	0.01	–0.13	–0.13
Philippines	0.008	0.00	–0.17	–0.17
Malaysia	0.005	0.00	–0.12	–0.12
Borneo	0.004	0.00	–0.14	–0.14
Java	0.0	0.00	–0.12	–0.12
Average	0.03	0.018	–0.11	–0.09

^a Results scaled to NO_x emission pulses of 0.1 Tg N.

^b Highest daily mean excess mixing ratio.

Table 4Peak ozone and time-integrated ozone responses at Mace Head, Ireland to North American NO_x emission pulses emitted in January

Region	Latitude	Longitude	Peak O ₃ response, ppb ^{a,b}	Time-integrated ozone response, ^a ppb months		
				Positive phase	Negative phase	Net
Washington–Oregon	40°–50°	130°–120°	1.05	0.54	–0.08	0.45
Idaho–Utah		120°–110°	3.47	0.56	–0.03	0.53
Montana–Nebraska		110°–100°	0.63	0.20	–0.03	0.17
Minnesota–Iowa		100°–90°	0.65	0.30	–0.03	0.27
Ontario–Ohio		90°–80°	1.57	0.34	–0.02	0.32
Quebec–New York		80°–70°	1.72	0.40	–0.04	0.35
New Brunswick		70°–60°	1.22	0.47	–0.07	0.40
Newfoundland		60°–50°	1.44	0.61	–0.09	0.52
California	30°–40°	130°–120°	2.11	0.51	–0.08	0.43
Nevada–Arizona		120°–110°	2.55	0.33	–0.02	0.31
Colorado–Texas		110°–100°	0.25	0.19	–0.02	0.17
Kansas–Mississippi		100°–90°	0.36	0.18	–0.03	0.14
Kentucky–Georgia		90°–80°	0.44	0.25	–0.04	0.20
Washington DC–Carolina		80°–70°	0.63	0.36	–0.07	0.29
Mexico 1	20°–30°	120°–110°	0.10	0.05	–0.05	0.01
Mexico 2		110°–100°	0.28	0.16	–0.02	0.13
Texas		100°–90°	0.41	0.22	–0.05	0.17
Florida		90°–80°	0.64	0.29	–0.08	0.21
Mexico 3	10°–20°	110°–100°	0.61	0.08	–0.11	–0.03
Mexico 4		100°–90°	0.14	0.08	–0.08	0.00
Honduras		90°–80°	0.22	0.13	–0.11	0.03
Average			0.98	0.30	–0.06	0.24

^a Results for NO_x emission pulses of 0.1 Tg N.^b Highest daily mean excess mixing ratio.

Time-integrated responses also showed significant seasonal variations. The NO_x-driven positive responses decreased markedly from January to July by a factor of 2–3 for the grid-squares to the west of the Rocky Mountains. Increases were found for the grid-squares along the east coast of North America. The CH₄-driven negative phase responses increased markedly from January to July. As a consequence, cancellation grew overall, leaving net time-integrated responses smaller, with eight grid-squares showing net negative responses in July compared to two grid-squares in January.

3.3. Spatial variations in source–receptor relationships across Europe

In this section, results are presented which illustrate the influence of NO_x emission pulses on O₃ levels at 20 additional receptor locations across Europe. The locations chosen were all rural ozone monitoring sites in the European Monitoring and Evaluation Programme (EMEP) network (see Table 6 for details). At each receptor location, the O₃ responses from all 18 North American NO_x pulse experiments in the latitude range from 20°–50° N for July (Table 5) were summed, to produce a grand total response at each receptor to North American NO_x emissions; this assumes each experiment is independent and the responses can be added linearly as discussed above (see Table 2). A 30-day rolling mean was then constructed for each location for 1st July onwards and the peak rolling mean responses at each receptor location are given in Table 6.

The locations in Table 6 have been ordered from west to east to highlight the gradient across Europe. Highest O₃ responses to the NO_x pulses emitted in North America were

found at the Mace Head, Ireland and Monte Vehlo, Portugal, locations on the Atlantic Ocean fringes of Europe. Responses steadily declined eastwards. At the location in the United Kingdom, the response had declined by about 10% and in Denmark, Germany, France and the Netherlands, it had declined by about 40%. At the central European

Table 5Peak ozone and time-integrated ozone responses at Mace Head, Ireland to North American NO_x emission pulses emitted in July

Region	Peak O ₃ response ppb ^{a,b}	Time-integrated ozone response, ^a ppb months		
		Positive phase	Negative phase	Net
Washington–Oregon	0.46	0.21	–0.10	0.11
Idaho–Utah	0.70	0.29	–0.11	0.19
Montana–Nebraska	1.41	0.37	–0.12	0.25
Minnesota–Iowa	1.23	0.46	–0.11	0.35
Ontario–Ohio	1.89	0.77	–0.13	0.65
Quebec–New York	1.73	0.88	–0.14	0.74
New Brunswick	2.17	1.16	–0.16	1.00
Newfoundland	3.17	1.21	–0.15	1.06
California	0.14	0.06	–0.15	–0.09
Nevada–Arizona	0.57	0.14	–0.10	0.04
Colorado–Texas	2.01	0.22	–0.10	0.09
Kansas–Mississippi	0.71	0.13	–0.14	0.06
Kentucky–Georgia	0.92	0.25	–0.10	0.15
Washington DC–Carolina	1.27	0.40	–0.12	0.28
Mexico 1	0.10	0.03	–0.16	–0.13
Mexico 2	0.41	0.09	–0.23	–0.15
Texas	0.40	0.06	–0.15	–0.10
Florida	0.36	0.06	–0.14	–0.08
Mexico 3	0.12	0.03	–0.40	–0.37
Mexico 4	0.14	0.04	–0.38	–0.33
Honduras	0.10	0.03	–0.38	–0.34
Average	0.95	0.33	–0.17	0.16

^a Results for NO_x emission pulses of 0.1 Tg N.^b Highest daily mean excess mixing ratio.

Table 6

Grand total ozone responses at 21 locations across Europe to 18 model experiments emitting pulses of NO_x in North America between 20°–50° N in July

Location	Country	Latitude and longitude ^a	Grand total O ₃ response, ^b ppb
Mace Head	Ireland	53°10', –09°30'	3.8
Monte Vehlo	Portugal	38°05', –08°48'	3.8
Harwell	UK	51°34', –01°19'	3.5
Tortosa	Spain	40°49', 00°29'	2.9
Revin	France	49°54', 04°38'	2.5
Kollumerwaard	Netherlands	53°20', 06°16'	2.4
Birkenes	Norway	58°23', 08°15'	2.6
Taenikon	Switzerland	47°28', 08°54'	3.0
Langenbrugge	Germany	52°48', 10°45'	2.0
Frederiksborg	Denmark	55°58', 12°20'	2.0
Montelibretti	Italy	42°06', 12°38'	3.3
Iskrba	Slovenia	45°34', 14°52'	2.6
Kostice	Czech Republic	49°35', 15°05'	2.0
Illmitz	Austria	47°46', 16°46'	1.5
Aspreveten	Sweden	58°48', 17°23'	1.7
K-puszta	Hungary	46°58', 19°35'	2.2
Preila	Lithuania	55°21', 21°04'	1.3
Jarczew	Poland	51°49', 21°59'	1.6
Starina	Slovakia	49°23', 22°16'	2.1
Lahemaa	Estonia	59°30', 25°54'	1.2
Virolahti	Finland	60°31', 27°41'	1.3
Average			2.4

^a Latitudes and longitudes taken from Hjellbrekke (2000).

^b Results for grand total of 18 NO_x emission pulses of 0.1 Tg N expressed as the highest rolling 30-day mean.

locations in Austria, Poland, the Czech Republic and Slovakia, the response was about one-half of that seen in Ireland and Portugal and in the east of Europe, the response was about one-third. There was evidence of higher responses at Montelibretti, Italy and Taenikon, Switzerland, two locations where orography appears to exert an important influence on the surface ozone responses. Stohl et al. (2002) have previously shown that North American emissions had their strongest impact on the surface in Europe in the Alps. Peak responses to North American NO_x emissions are thus lowest in the more polluted regions of central Europe where O₃ lifetimes are shortest due to photochemical activity. They are highest where in-flow from the North Atlantic is the strongest and travel times over land are the shortest, minimising losses due to dry deposition.

3.4. Mechanisms of intercontinental ozone formation and transport

To aid in the source–receptor analysis, the parcel-following capabilities of the STOCHEM model have been used to trace the pulses of NO_x and how they affect O₃ as they are transported from Asia to Mace Head. A detailed study was made of the air parcels involved in the January pulse experiment over the 'Japan' region. Although the NO_x emission pulse began on 1st January, excess O₃ was not found in air parcels arriving at Mace Head until nearly 2 weeks had elapsed. Excess ozone was then found for a period of over 5 weeks. For example an air parcel that passed over the 'Japan' region around 25th January rapidly

generated 3 ppb excess ozone as it travelled west out over the Pacific Ocean. This air parcel then showed a steady decline in excess O₃ as it travelled at 3–5 km altitude across the Pacific Ocean, then over the North American continent and Atlantic Ocean before descending to the surface at the Atlantic Ocean coast of Ireland. By the time the parcel reached Mace Head, the excess O₃ has decreased to about 1 ppb, with the trajectory across the Pacific, North America, and the North Atlantic being direct and rapid, taking only 15 days. It is notable that the flow occurred in the mid-troposphere at an altitude of around 3–5 km. This result contrasts with the generally accepted mechanism for intercontinental transport from Asia, which is thought to involve frontal uplifting over the Pacific coast of Asia and then rapid horizontal transport in the upper troposphere (Wild and Akimoto, 2001). The difference between our study and that of Wild and Akimoto is that they considered the export of O₃ to the global troposphere at all levels, whilst we consider only air that reaches the boundary layer over Europe.

A total of 1200 air parcels were analysed that had passed within the boundary layer close to Mace Head within 1 yr. Of these, 81 had received emissions whilst within the North American boundary layer during the previous 20 days. The trajectories of all 81 air parcels stayed below about 4 km (600 hPa) as they crossed the North Atlantic Ocean. The importance of transport in the lower free troposphere has been noted by Owen et al. (2006) in their analysis of the mechanisms of North American pollutant transport to the Azores.

4. Discussion and conclusions

We have performed a series of month-long pulse experiments with a patchwork design using a global Lagrangian chemistry-transport model to assess the source–receptor relationships that link surface NO_x emissions in Asia and North America with surface ozone in Europe. Our results demonstrate how NO_x emission pulses emitted in one continent generate surface O₃ responses in another. Furthermore, ozone responses at a given location in Europe vary by up to three orders of magnitude depending on the location of the NO_x emission pulse. Lower responses were characterised for NO_x emission pulses emitted during summer conditions for Asia with the reverse often found for North America. The net impact of NO_x emissions on European ozone levels is determined by a balance between the direct transport of ozone and the indirect effect of the methane removal. The direct transport of ozone is greatest for emissions from a similar latitude to Europe, greater for emissions from North America than Asia and greater in winter than in summer. The indirect effect on methane is greatest for emissions in the tropics and in the boreal summer when methane removal is most efficient.

It is of interest to compare the results reported here for the series of hypothetical emission pulse experiments with those from step-change experiments that have been reported already in the literature. The transient O₃ response to a step-change in NO_x emissions can be deconvolved into a series of pulse responses and, vice versa, a step-change response can be constructed from

a series of pulse responses. Thus a step-change response can be assessed from the model experiments performed here by building up the responses from pulse experiments, each delayed by 1 month. Assuming that the pulses from the 21 emission locations act independently, that their responses are each in their linear range and are independent of sign, as discussed above (see Table 2), then the response to a continental step-change in NO_x emissions of $21 \times 0.1 \times 12 = 25.2 \text{ Tg N yr}^{-1}$ can be assessed. Fig. 3 presents the build-up of the O_3 responses at Mace Head to the step-change in North American (top curves) and Asian (bottom curves) NO_x emissions, together with the 12-month running mean responses (smooth curves). The responses to both step-changes steadily decline with time as the impact of the indirect effect on CH_4 builds up. Over the 1st year, the average responses amounted to 6.1 ± 1 and 1.3 ± 0.3 ppb, respectively, for step-changes in North America and Asia. Using Table 6, assuming linearity and independence of sign, these responses amounted to 0.21 ± 0.04 and 0.06 ± 0.01 ppb, respectively, for 20% step-change increases in North American and Asian NO_x emissions.

In the Task Force on the Hemispheric Transport of Air Pollution TF HTAP intercomparison exercise (Keating and Zuber, 2007), 20 global chemistry-transport models (including STOCHEM) each performed a step-change experiment involving a 20% reduction in man-made NO_x emissions from each of Europe, North America, South Asia and East Asia for the year 2001, with fixed methane levels. The multi-model annual mean decrease in surface ozone over Europe amounted to 0.22 ± 0.06 ppb for

a step-change in North American emissions and 0.04 ± 0.02 – 0.08 ± 0.02 ppb, respectively, for step-changes in South and east Asian NO_x emissions. Bearing in mind the range over the 20 model studies, the agreement between the present results and those from Keating and Zuber (2007) is excellent. It is concluded that continental step-change experiments hide an exceedingly large amount of spatial variation as revealed by our patchwork experimental design. The fact that methane is kept fixed in the HTAP experiments also hides the longer-term impacts of NO_x that occur via a reduction in methane. In some cases we find significant differences between the initial response compared to the equilibrium response (i.e. after ~ 50 yr) (Fig. 3). This is especially true for NO_x emissions from lower latitudes, where the equilibrium response is negative, i.e. NO_x emissions from these sites ultimately lead to reductions in European ozone.

In this study, the coupling between the enhanced ozone and OH production led to changing methane and ozone distributions and hence the representation of an important coupling between these major radiatively active trace gases. Treatment of the feedback on methane has led to an apparent reduction in the magnitude of intercontinental source–receptor relationships linking surface NO_x emissions in one continent with surface ozone in another, when a long-term view is taken, see Fig. 3. Pulse experiments can reveal variations in source–receptor relationships due to geographical and seasonal factors as well as mechanistic details involving the altitude level at which intercontinental transport occurs and the chemical processes involved.

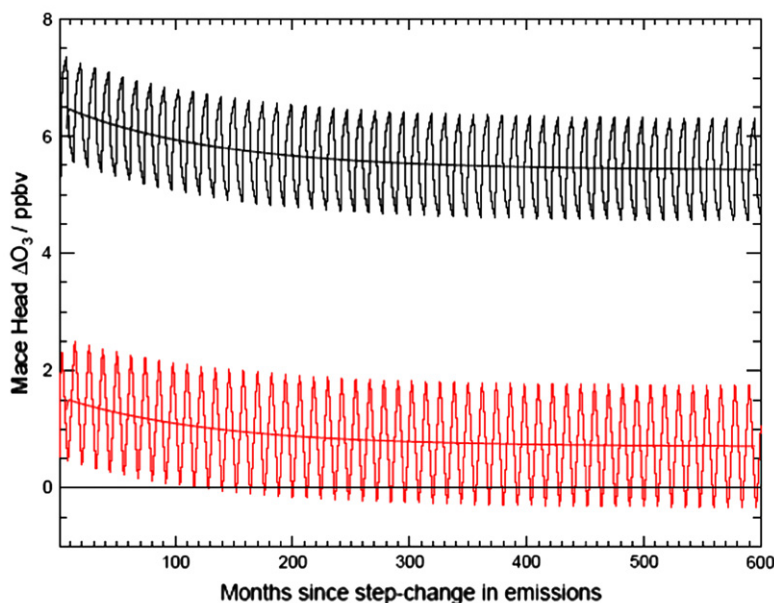


Fig. 3. Estimated surface ozone responses (ppb) at Mace Head to step-changes in North American (upper curves) and Asian (lower curves) NO_x emissions, shown on a monthly (strongly varying) and rolling 12-month average (smoothed curve) basis, out to 50 years following the step-change, when equilibrium has been reached. The step-change responses were constructed by summing the responses from multiple month-long pulse experiments, and extrapolating the responses beyond the end of each experiment assuming a simple exponential decay with an e-folding timescale of 11 yr. Pulse experiments for months between January and July were estimated assuming linear interpolation in time. The responses shown have not been normalised, and represent the responses to total NO_x emission increases of $25.2 \text{ Tg N yr}^{-1}$ from each continent (see text for details).

In these calculations, we have begun the process of assessing the source–receptor relationships that link surface NO_x emissions in North America and Asia with surface ozone in Europe. In this way, it should be possible to examine the likely benefits of ozone precursor emission controls in North America and Asia from reductions in ozone levels across Europe and their possible contribution to meeting ozone air quality targets and guidelines. It is likely that any benefits within Europe will depend on the magnitude and geographical location of any NO_x emission controls. This will mean that there may well be important policy issues of international cost-effectiveness as well as of the likely benefits that may accrue within the source continent. These are, however, initial calculations and further detailed studies using a range of differently formulated global models are needed, not only on the effects of NO_x emission controls, but also on the controls on the other tropospheric O₃ precursor gases: CH₄ (see, for example, Fiore et al., 2002; West et al., 2006), carbon monoxide and VOCs.

Acknowledgements

RGD, WJC and MGS were supported by the Air and Environmental Quality Division of the United Kingdom, Department for Environment, Food and Rural Affairs (Defra) under contract AQ0902. WJC and MGS were additionally supported by the joint Defra and Ministry of Defence (Mod) programme, (Defra) GA01101 (Mod) CBC/2B0417 Annex C5. DSS and RMD thank the Natural Environment Research Council for support from grant NE/D012538/1.

References

- Arndt, R.L., Carmichael, G.R., 1995. Long-range transport and deposition of sulphur in Asia. *Water, Air and Soil Pollution* 85, 2283–2288.
- Auvray, M., Bey, I., 2005. Long-range transport to Europe: seasonal variations and implications for the European ozone budget. *Journal of Geophysical Research* 110, D11303. doi:10.1029/2004JD005503.
- Bartnicki, J., 2000. Nonlinear Effects in the Source Receptor Matrices Computed with the EMEP Eulerian Acid Deposition Model. EMEP/ MSC-W Note 4/2000. Norwegian Meteorological Institute, Oslo, Norway.
- Charron, A., Plaisance, H., Sauvage, S., Coddeville, P., Gallo, J.-C., Guillermo, R., 2000. A study of source–receptor relationships influencing the acidity of precipitation collected at a rural site in France. *Atmospheric Environment* 34, 3665–3674.
- Cofala, J., Amann, M., Klimont, Z., Kupiainen, K., Hoglund-Isaksson, L., 2007. Scenarios of global anthropogenic emissions of air pollutants and methane until 2030. *Atmospheric Environment* 41, 8486–8499.
- Collins, W.J., Derwent, R.G., Johnson, C.E., Stevenson, D.S., 2000. The impact of human activities on the photochemical production and destruction of tropospheric ozone. *Quarterly Journal of the Royal Meteorological Society* 126, 1925–1951.
- Collins, W.J., Stevenson, D.S., Johnson, C.E., Derwent, R.G., 1997. Tropospheric ozone in a global-scale three-dimensional Lagrangian model and its response to NO_x emission controls. *Journal of Atmospheric Chemistry* 26, 223–274.
- Collins, W.J., Stevenson, D.S., Johnson, C.E., Derwent, R.G., 1999. The role of convection in determining the budget of odd hydrogen in the upper troposphere. *Journal of Geophysical Research* 104, 26927–26941.
- Commission of the European Communities, 2005. Proposal for a Directive of the European Parliament and of the Council on Ambient Air Quality and Cleaner Air for Europe. COM(2005) 447 final. Commission of the European Communities, Brussels, Belgium.
- Cooper, O.R., Moody, J.L., Parrish, D.D., Trainer, M., Ryerson, T.B., Holloway, J.S., Hubler, G., Fehsenfeld, F.C., Oltmans, S.J., Evans, M.J., 2001. Trace gas signatures of the airstreams within North Atlantic cyclones: case studies from the North Atlantic Regional Experiment (NARE'97) aircraft intensive. *Journal of Geophysical Research* 106, 5437–5456.
- Dentener, F., Stevenson, D., Cofala, J., Mechler, R., Amann, M., Bergamaschi, P., Raes, F., Derwent, R., 2005. The impact of air pollutant and methane emission controls on tropospheric ozone and radiative forcing: CTM calculations for the period 1990–2030. *Atmospheric Chemistry and Physics* 5, 1731–1755.
- Derwent, R.G., Collins, W.J., Johnson, C.E., Stevenson, D.S., 2001. Transient behaviour of tropospheric ozone precursors in a global 3-D CTM and their indirect greenhouse effects. *Climatic Change* 49, 463–487.
- Derwent, R.G., Stevenson, D.S., Collins, W.J., Johnson, C.E., 2004. Inter-continental transport and the origins of the ozone observed at surface sites in Europe. *Atmospheric Environment* 38, 1891–1901.
- Derwent, R.G., Simmonds, P.G., O'Doherty, S., Stevenson, D.S., Collins, W.J., Sanderson, M.G., Johnson, C.E., Dentener, F., Cofala, J., Mechler, R., Amann, M., 2006. External influences on Europe's air quality: methane, carbon monoxide and ozone from 1990 to 2030 at Mace Head, Ireland. *Atmospheric Environment* 40, 844–855.
- Fiore, A.M., Jacob, D.J., Field, B.D., Streets, D.G., Fernandes, S.D., Jang, C., 2002. Linking ozone pollution and climate change: the case for controlling methane. *Geophysical Research Letters* 29, 1919. doi:10.1029/2002GL015601.
- Gebhart, K.A., Malm, W.C., Flores, M., 2000. A preliminary look at source–receptor relationships in the Texas–Mexico border area. *Journal of the Air and Waste Management Association* 50, 858–868.
- Hjellbrekke, A.-G., 2000. Ozone Measurements 1998. EMEP/CCC-Report 5/2000. Norwegian Institute for Air Research, Kjeller, Norway.
- Keating, T., Zuber, A., 2007. Hemispheric Transport of Air Pollutants 2007. Convention on Long-range Transboundary Air Pollution. UN ECE, Geneva, Switzerland.
- Lelieveld, J., et al., 2002. Global air pollution crossroads over the Mediterranean. *Science* 298, 794–799.
- Li, Q., Jacob, D.J., Park, R., Wang, Y., Heald, C.L., Hudman, R., Yantosca, R.M., 2005. North American pollution outflow and the trapping of convectively lifted pollution by upper-level anticyclone. *Journal of Geophysical Research* 110, D10301. doi:10.1029/2004JD005039.
- Lin, X., Trainer, M., Liu, S.C., 1988. On the non-linearity of the tropospheric ozone production. *Journal of Geophysical Research* 93, 15879–15888.
- Owen, R.C., Cooper, O.R., Stohl, A., Honrath, R.E., 2006. An analysis of the mechanisms of North American pollutant transport to the central North Atlantic lower free troposphere. *Journal of Geophysical Research* 111, D23558. doi:10.1029/2006JD007062.
- Parrish, D.D., Holloway, J.S., Trainer, M., Murphy, P.C., Forbes, G.L., Fehsenfeld, F.C., 1993. Export of North American ozone pollution to the North Atlantic Ocean. *Science* 259, 1436–1439.
- Prinn, R.G., Weiss, R.F., Miller, B.R., Huang, J., Aleya, F.N., Cunnold, D.M., Fraser, P.J., Hartley, D.E., Simmonds, P.G., 1995. Atmospheric trends and lifetime of CH₃CCl₃ and global OH concentrations. *Science* 269, 187–192.
- Simmonds, P.G., Derwent, R.G., Manning, A.L., Spain, G., 2004. Significant growth in surface ozone at Mace Head, Ireland, 1987–2003. *Atmospheric Environment* 38, 4769–4778.
- Stevenson, D.S., Doherty, R.M., Sanderson, M.G., Collins, W.J., Johnson, C.E., Derwent, R.G., 2004. Radiative forcing from aircraft NO_x emissions: mechanisms and seasonal dependence. *Journal of Geophysical Research* 109, D17307. doi:10.1029/2004JD004759.
- Stevenson, D.S., Solberg, S., Lindskog, A., Derwent, D., 2002. Comparison of surface ozone at European sites with a global model. In: Midgley, P. M., Reuther, M. (Eds.), *Proceedings of the EUROTRAC-2 Symposium 2002: Transport and Transformation in the Troposphere*. Margraf Verlag, Weikersheim, Germany.
- Stevenson, D.S., et al., 2006. Multimodel ensemble simulations of present-day and near-future tropospheric ozone. *Journal of Geophysical Research* 111, D08301. doi:10.1029/2005JD006338.
- Stohl, A., 1996. Trajectory statistics – a new method to establish source–receptor relationships of air pollutants and its application to the transport of particulate sulphate in Europe. *Atmospheric Environment* 30, 579–587.
- Stohl, A., 2001. A 1-year Lagrangian 'climatology' of airstreams in the Northern Hemisphere troposphere and lowermost stratosphere. *Journal of Geophysical Research* 106, 7263–7280.
- Stohl, A., Trickl, T., 1999. A textbook example of long-range transport: simultaneous observation of ozone maxima of stratospheric and

- North American origin in the free troposphere over Europe. *Journal of Geophysical Research* 104, 30445–30462.
- Stohl, A., Eckhardt, S., Forster, C., James, P., Spicinger, N., 2002. On the pathways and timescales of intercontinental air pollution transport. *Journal of Geophysical Research* 107, 4684. doi:10.1029/2001JD001396.
- Venkatram, A., Karamchandani, P., 1986. Source–receptor relationships. A look at acid deposition modelling. *Environmental Science and Technology* 20, 1084–1091.
- West, J.J., Fiore, A.M., Horowitz, L.W., Mauzerall, D.L., 2006. Global health benefits of mitigating ozone pollution with methane emission controls. *Proceedings of the National Academy of Sciences of the United States of America* 103, 3993–3998.
- Wild, O., Akimoto, H., 2001. Intercontinental transport of ozone and its precursors in a three-dimensional global CTM. *Journal of Geophysical Research* 106, 27729–27744.
- Wild, O.M., Prather, M.J., Akimoto, H., 2001. Indirect long-term global radiative cooling from NO_x emissions. *Geophysical Research Letters* 28, 1719–1722.